

# ESTIMATING THE SABINE ABSORPTION COEFFICIENT OF FIBROUS MATERIALS FOR VARIOUS BACKING CONDITIONS

Cheol-Ho Jeong

*Acoustic Technology, Department of Electrical Engineering, Technical University of Denmark, Denmark*  
email: [chj@elektro.dtu.dk](mailto:chj@elektro.dtu.dk)

Since absorber manufacturers cannot provide the absorption coefficients for all possible mounting conditions, acousticians have difficulties knowing the absorption characteristics of their own configurations. This paper aims to predict the Sabine absorption coefficient for various mounting conditions by extracting the air flow resistivity of the test specimen and the frequency-dependent effect of the chamber on the measured absorption coefficients. Two homogeneous fibrous absorbers are measured for experimental validation, showing good agreements between the predictions and measurements.

**Keywords:** Fibrous absorbers, Sabine absorption coefficient, flow resistivity extraction

---

## 1. Introduction

Fibrous ceiling absorbers are often backed by an air cavity depending on required low frequency acoustic demands because they generally have insufficient absorption at low frequencies when mounted directly on a rigid surface [1]. The overall depth of the ceiling system including the absorber is found to vary from 20 to 100 cm in 17 Swedish classrooms [2]. However, the absorption characteristics of commercial products are presented for a few mounting conditions in their product database, as ISO 354 absorption measurements [3] for various mounting conditions can easily take a lot of time and effort. Therefore, the aim of this paper is to predict the absorption property of homogeneous fibrous materials for many air backing conditions from absorption measurement data performed with a given backing condition. Such a numerical procedure is a good compromise because users can predict the absorption of any air backing conditions chosen for their own purposes.

The Sabine absorption coefficient [4],  $\alpha_{\text{Sab}}$ , is the statistical absorption coefficient deduced from reverberation time measurements via the Sabine equation in accordance with ISO 354. The calculation of  $\alpha_{\text{Sab}}$  is based on the diffuse field assumption. However, actual measurement conditions violate the diffuse field assumption, particularly when a highly absorbing specimen is installed, due to a non-uniform surface absorption distribution [5].  $\alpha_{\text{Sab}}$  is also known to vary with the specimen size due to diffraction by the specimen edge [6-8]. Many round robin tests reported a poor inter-chamber reproducibility, indicating that  $\alpha_{\text{Sab}}$  depends largely on the reverberation chamber [9-11]. Some chambers systematically overestimate, while others underestimate the absorption coefficient. Therefore, translating  $\alpha_{\text{Sab}}$  between test chambers is a nearly impossible task without knowing the exact diffuseness conditions. In this regard, the main scope of this study is limited to predictions of  $\alpha_{\text{Sab}}$  for other mounting conditions, as if the same material is measured in the same chamber. The most practical application of the suggested method is to predict the absorption coefficients for other air backing or other thickness cases with known absorption data for a given mounting condition.

Several conversion methods between acoustical properties have been suggested [12-14]. Recently Jeong proposed a method to inversely estimate the surface impedance and flow resistivity from  $\alpha_{\text{Sab}}$  based on an equivalent fluid model to estimate the random incidence absorption coefficient.

cient [13]. A similar conversion method was used to investigate the reproducibility of the converted random incidence absorption coefficient using a frequency-independent room factor [14]. This study introduces a new frequency-dependent diffuseness factor to extract the flow resistivity of the test specimen from an arbitrary mounting condition.

## 2. Porous absorption model

Throughout the study, the material production variability is assumed to be negligible. The basic assumption is that one can accurately predict  $\alpha_{Sab}$  with two independent corrections: a finite size correction and room's diffuseness correction [14]. The former correction can account for edge diffraction from a finite specimen, whereas the latter can account for the inter-chamber variation in  $\alpha_{Sab}$  shown in the round robin tests [9-11]. The room's diffuseness correction can include many factors, e.g., room geometry and diffuser setting, mounting and frame around the sample, and measurement method, etc.<sup>14</sup> The main challenge concerning the diffuseness correction is that there are no well-established methods to compensate for the individual diffuseness condition, and therefore a frequency-independent correction was initially suggested in Ref. [14]. This frequency-independent correction, however, is a crude approximation because the diffuseness varies with frequency and the absorption characteristic of the specimen. In this study, a frequency-dependent diffuseness correction is suggested based on recent round robin data [10], which is assumed to hold good for porous materials.

The frequency dependence of the inter-chamber variation in  $\alpha_{Sab}$  is extracted from a recent round robin test, where 2 porous specimens were measured in 13 reverberation chambers.<sup>10</sup> The mean and standard deviation (STD) of  $\alpha_{Sab}$  are calculated from the 13 measurements in each third octave band in Figs. 1(a-b). The inter-chamber STD indicates how much the chamber biases the absorption measurement, on average. STDs of two quite different porous absorbers differ largely at low frequencies in Fig. 1(b) [10, 14], mainly because  $\alpha_{Sab}$  differs a lot in Fig. 1(a). When STD is normalized by its mean  $\alpha_{Sab}$ , the relative standard deviations (RSDs) for the two absorbers become quite similar in Fig. 1(c). These two RSDs are averaged and named RSD(f), which serves as a pre-defined frequency-dependent trend of the chamber's influence on the measured absorption of porous absorbers. With this newly suggested correction, the flow resistivity as a material property of the sample is extracted (Step 1 in Sec. 2.1). Then, the absorption coefficient for another mounting condition is predicted via Miki's model and the same diffuseness correction based on the extracted flow resistivity information (Step 2 in in Sec. 2.2).

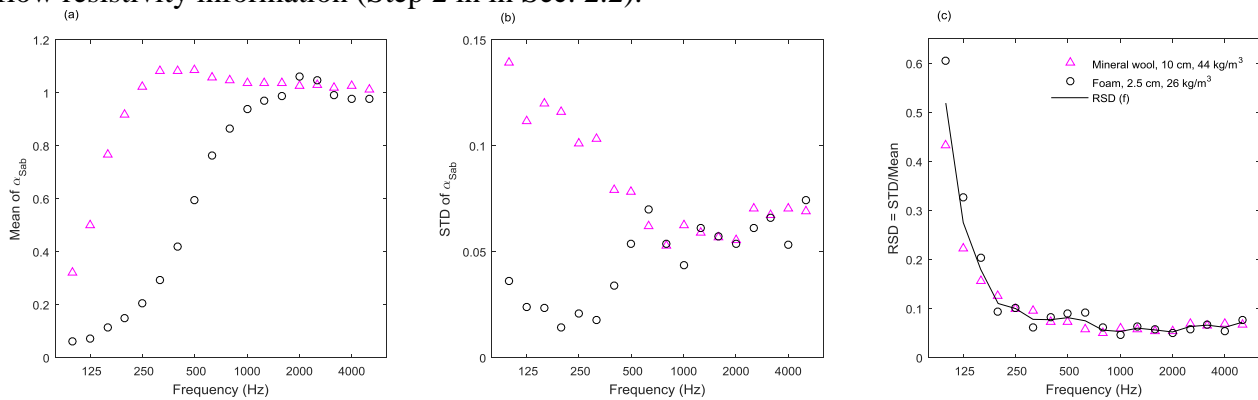


Figure 1. (a)  $\alpha_{Sab}$  averaged over the chamber,<sup>10</sup> (b) Inter-chamber STD of  $\alpha_{Sab}$ , (c) RSD of  $\alpha_{Sab}$ .

### 2.1 Step 1: Extracting the flow resistivity based on an equivalent fluid model

The flow resistivity,  $\sigma$ , is one of the most important material parameters to estimate the absorption of fibrous absorbers. The best known equivalent fluid model is the model of Delany and Bazley [15], with a number of modifications available.<sup>16</sup> In this study, the model of Miki [16] is consistently used, which was constructed based on Delany-Bazley's data in a limited frequency range be-

tween  $0.01\sigma$  and  $\sigma$ . Once the characteristic impedance,  $Z_c$  and the propagation constant,  $k_t$  are computed by Miki's model, the surface impedance for oblique incidence is expressed as [17]

$$Z_w(f, \theta) = Z_c k \left( -j Z_{|x=d} \cot(k_x d) + Z_c \frac{k}{k_x} \right) / \left[ k_x \left( Z_{|x=d} - j Z_c \frac{k}{k_x} \cot(k_x d) \right) \right], \quad (1)$$

where  $\theta$  is the incidence elevation angle,  $k$  is the wavenumber in air,  $k_x$  is the normal component of the transmitted wavenumber  $k_t$  ( $k_x = \sqrt{k_t^2 - k^2 \sin^2(\theta)}$ ), and  $d$  is the absorber thickness. For a rigid backing,  $Z_{|x=d} = \infty$ . For an air cavity backing,  $Z_{|x=d} = -j(\rho_o c_o k_o / k_x) \cot(k_o d_o \cos \theta)$ , where  $d_o$  is the air cavity depth.

To predict  $\alpha_{Sab}$ , a size- and room- corrected absorption coefficient,  $\alpha_{size\&room}$ , was suggested [14, 18], which assumes a frequency-independent effect of the chamber on the measured absorption as follows:

$$\alpha_{size\&room}(f) = 2 \int_0^{\pi/2} \frac{4 \operatorname{Re}(Z_w(f, \theta))}{|Z_w(f, \theta) + \bar{Z}_r^*(f, \theta)|^2} \sin(\theta) d\theta + \alpha_{room} = \alpha_{size}(f) + \alpha_{room}. \quad (2)$$

Here,  $\bar{Z}_r(f, \theta)$  is the average radiation impedance of a finite specimen over the azimuth angle<sup>18</sup> and  $\alpha_{room}$  is the frequency-independent room factor. A new frequency-dependent correction is introduced as

$$\alpha_{size\&diff}(f) = \alpha_{size}(f) + \alpha_{diff} \frac{RSD(f) \cdot \alpha_{size}(f)}{\overline{RSD(f) \cdot \alpha_{size}(f)}}. \quad (3)$$

Here,  $RSD(f) \cdot \alpha_{size}(f) / \overline{RSD(f) \cdot \alpha_{size}(f)}$  means the normalized, predefined, frequency-dependent effect of the test chamber on the measured absorption, with  $\overline{[\bullet]}$  being the average over the frequency of interest. Therefore,  $\alpha_{diff}$  is interpreted as a single-valued overestimation or underestimation by the test chamber based on the frequency-dependent correction, which is an equivalent concept to  $\alpha_{room}$  in Eq. (2). To find the optimal  $\sigma$  and  $\alpha_{diff}$  (or  $\alpha_{room}$ ), the error function to be minimized is defined as the summation of the absolute difference between  $\alpha_{Sab}$  and  $\alpha_{size\&diff}$  (or  $\alpha_{size\&room}$ ) over the frequency range as follows:

$$e_{size\&diff}(\sigma, \alpha_{diff}) = \sum_{f=f_{min}}^{f_{max}} |\alpha_{Sab}(f) - \alpha_{size\&diff}(\sigma, \alpha_{diff}, f)|, \quad (4a)$$

$$e_{size\&room}(\sigma, \alpha_{room}) = \sum_{f=f_{min}}^{f_{max}} |\alpha_{Sab}(f) - \alpha_{size\&room}(\sigma, \alpha_{room}, f)|. \quad (4b)$$

One can directly minimize the error function as performed in Ref. [14] or simply explore the error distribution for a typical range of  $\sigma$  and  $\alpha_{diff}$ . The latter approach is chosen in this study to clearly visualize the error distribution.

## 2.2 Step 2: Estimating $\alpha_{size\&diff}$ for other mounting conditions

Once the flow resistivity value that minimizes the error function is found,  $\alpha_{size\&diff}$  for another mounting condition is predicted according to Eq. (3). First,  $Z_c$  and  $k_t$  are estimated by Miki's model, and then a new surface impedance is estimated by Eq. (1). Note that the correct backing impedance,  $Z_{|x=d}$ , for the new mounting condition should be computed.

## 3. Ecophon Industry Modus

Ecophon Industry<sup>TM</sup> Modus was a 10 cm thick glass wool absorber with a density of 26.5 kg/m<sup>3</sup>. Its flow resistivity was measured to be 12.9 kNsm<sup>-4</sup> according to ISO 9053 [19] by Matelys and 10.9 kNsm<sup>-4</sup> by Ecophon. Two mounting conditions were measured in a rectangular reverberation chamber of a volume of 214 m<sup>3</sup> with six panel diffusers (Chamber 1): Rigid backing (Rigid) and 10 cm air cavity backing (Cavity). The measured absorber size was 10.8 m<sup>2</sup>. The 1/3 octave bands used

for the optimization range from 125 Hz to 5 kHz, as the 100 Hz band is excluded due to a low value of its flow resistivity and the respective limitation of Miki's model.

Four contour plots of the error function are shown in Fig. 3. From Rigid1 condition,  $(\sigma, \alpha_{room})$  are found to be  $(16.4 \text{ kNsm}^{-4}, 0.045)$  with the frequency-independent correction, whereas the optimum parameters,  $(\sigma, \alpha_{diff})$ , are  $(12.6 \text{ kNsm}^{-4}, 0.040)$  with the frequency-dependent correction shown in Figs. 3(a-b). In Figs. 3(c-d), the optimized parameters from Cavity1 condition are  $(\sigma, \alpha_{room}) = (26.4 \text{ kNsm}^{-4}, 0.085)$  and  $(\sigma, \alpha_{diff}) = (9.6 \text{ kNsm}^{-4}, 0.050)$ , respectively. Note that the optimized values are global minima in the typical  $\sigma$  and  $\alpha_{diff}$  range in Fig. 3. The  $\sigma$  prediction with  $\alpha_{diff}$  agrees better with the measured  $\sigma$  of  $12.9 \text{ kNsm}^{-4}$  or  $10.9 \text{ kNsm}^{-4}$  than that with  $\alpha_{room}$ . Based on the optimized sets of  $(12.6 \text{ kNsm}^{-4}, 0.04)$  and  $(9.6 \text{ kNsm}^{-4}, 0.05)$  extracted from Figs. 3(b,d),  $\alpha_{size\&diff}$  and  $\alpha_{Sab}$  are compared in Fig. 4. The absolute differences between  $\alpha_{size\&diff}$  and  $\alpha_{Sab}$  per frequency band for Rigid1 and Cavity1 condition are smaller than 0.04.

Considering the fact that the flow resistivity values of fibrous materials vary from  $2 \text{ kNsm}^{-4}$  to  $200 \text{ kNsm}^{-4}$  [20], the present study investigates a relatively low flow resistivity example. There are several cautions when applying the proposed prediction. First, some absorber manufactures present only the practical absorption coefficient,  $\alpha_p$ , averaged in the octave band, approximated in steps of 0.05, and truncated in order not to exceed unity. Therefore, the correct shape of the absorption coefficient may not be preserved in  $\alpha_p$ , and thus  $\alpha_{Sab}$  is preferred to  $\alpha_p$ . If absorber manufacturers can provide the flow resistivity, the flow resistivity does not need to be optimized. Second, absorption predictions for absorbers having higher flow resistivity values are expected to be less accurate. For example, Miki's model is not sufficiently accurate below  $0.01\sigma$  [21], which amounts to 500 Hz for a flow resistivity of  $50 \text{ kNsm}^{-4}$ . Accordingly, some low frequency absorption data should be discarded for the optimization process, which includes the most notable and useful difference between the two different backing conditions. Another porous absorber example with a high flow resistivity can be found in [22].

## 4. Conclusion

This study deals with a simple numerical prediction method of the Sabine absorption coefficient for homogeneous fibrous materials from one to other mounting conditions. From the measured Sabine absorption data for a given mounting condition, one can extract the flow resistivity of the test specimen and the frequency-dependent diffuseness correction term, and then re-calculate  $\alpha_{size\&diff}$  for other mounting conditions. The fibrous absorber example shows that the prediction error is no larger than 0.04.

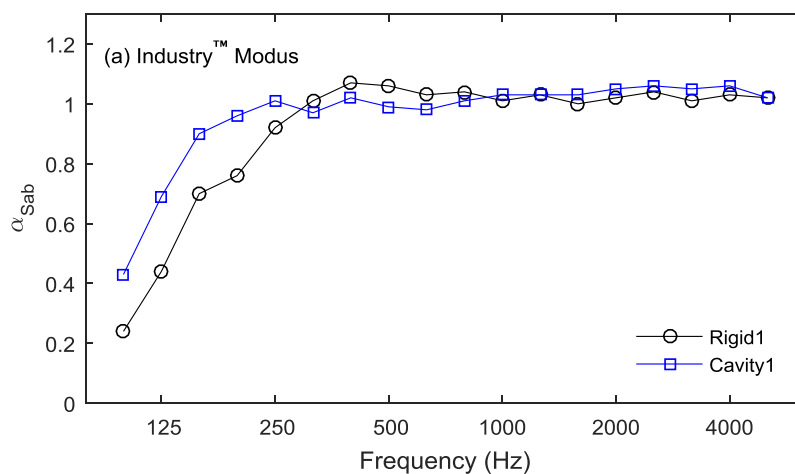


Figure 2. Sabine absorption coefficients of Ecophon Industry™ Modus.

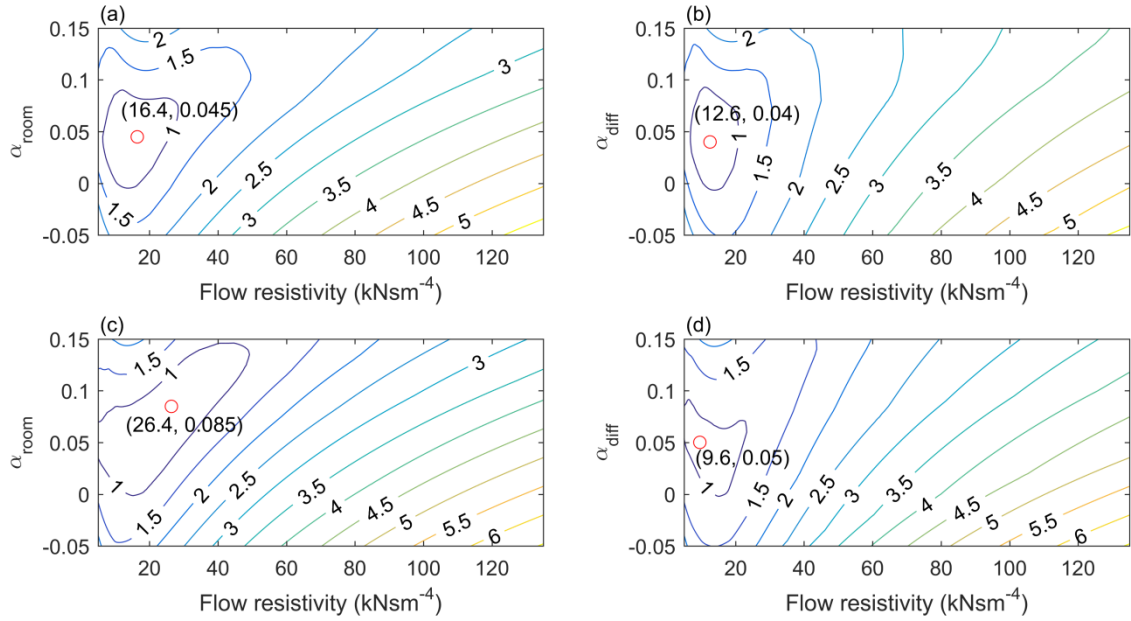


Figure 3. The error function in Eq. (4) by varying the flow resistivity and diffuseness factor.  
 (a) Rigid1 with  $\alpha_{room}$ , (b) Rigid1 with  $\alpha_{diff}$ , (c) Cavity1 with  $\alpha_{room}$ , (d) Cavity1 with  $\alpha_{diff}$ .

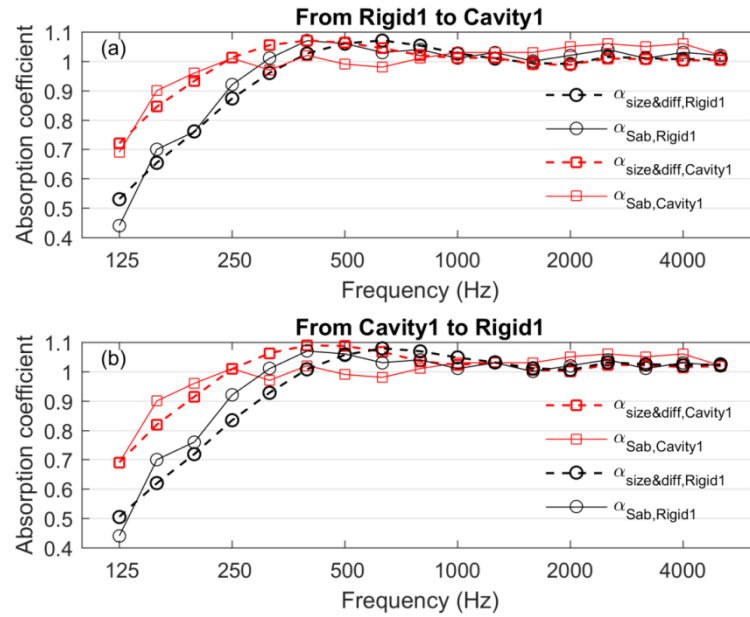


Figure 4. A comparison between  $\alpha_{size \& diff}$  and  $\alpha_{Sab}$  for Industry<sup>TM</sup> Modus.  
 (a) Conversion from Rigid1 to Cavity1 ( $\sigma$ ,  $\alpha_{diff}$ )=(12.6 kNsm<sup>-4</sup>, 0.04),  
 (b) Conversion from Cavity1 to Rigid1 ( $\sigma$ ,  $\alpha_{diff}$ )=(9.6 kNsm<sup>-4</sup>, 0.050).

## ACKNOWLEDGMENT

The author thanks Mélanie Nolan, DTU, for providing the absorption data.

## REFERENCES

- 1 Vigran, T. E. Building Acoustics, 1st edition ed, Taylor & Francis, London, (2008).
- 2 Nilsson, E. Room acoustic measures for classrooms, Proceedings of Internoise 2010, (2010).
- 3 Anon., ISO 354:2003, "Acoustics - Measurement of sound absorption in a reverberation room",
- 4 Morfey, C. Dictionary of acoustics, Academic Press, London, (2001).
- 5 Hodgson, M. When is Diffuse-Field Theory Applicable?, Appl. Acoust., 49, 197-207, (1996).
- 6 Thomasson, S.-I. On the absorption coefficient, Acustica, 44, 265-273, (1980).
- 7 Jeong, C.-H. A correction of random incidence absorption coefficients for the angular distribution of acoustic energy under measurement conditions, J. Acoust. Soc. Am., 125, 2064-2071, (2009).
- 8 Jeong, C.-H. Non-uniform sound intensity distributions when measuring absorption coefficients in reverberation chambers using a phased beam tracing, J. Acoust. Soc. Am., 127, 3560-3568, (2010).
- 9 Kosten, C. W. International comparison measurement in the reverberation room, Acustica, 10, 400-411, (1960).
- 10 Vercammen, M. Improving the accuracy of sound absorption measurement according to ISO 354, Proceedings of the International Symposium on Room Acoustics, (2010).
- 11 Nolan, M., Vercammen, M., Jeong, C.-H. and Brunskog, J. The use of a reference absorber for absorption measurements in a reverberation chamber, Proceedings of Forum Acusticum 2014, September 2014, (2014).
- 12 Rindel, J. H. An impedance model for estimating the complex pressure reflection factor, Forum Acusticum 2011, (2011).
- 13 Jeong, C.-H. Converting Sabine absorption coefficients to random incidence absorption coefficients, J. Acoust. Soc. Am., 133, 3951-3962, (2013).
- 14 Jeong, C.-H. and Chang, J.-H. Reproducibility of the random incidence absorption coefficient converted from the Sabine absorption coefficient, Acta Acustica united with Acustica, 101, 99-112, (2015).
- 15 Delany, M. E. and Bazley, E. N. Acoustical properties of fibrous absorbent materials, Appl. Acoust., 3, 105-116, (1970).
- 16 Miki, Y. Acoustical properties of porous materials - modifications of Delany-Bazley models, J. Acoust. Soc. Jp., 11, 19-28, (1990).
- 17 Allard, J.-F. and Atalla, N. Propagation of Sound in Porous Media: Modelling Sound Absorbing materials, 2nd Edition, John Wiley and Sons, London, (2009).
- 18 Jeong, C.-H. Sabine absorption coefficient predictions using different radiation impedances of a finite absorber Acta Acustica united with Acustica, 101 (4), 663-667, (2015).
- 19 Anon., ISO 9053:1991, "Acoustics - Materials for acoustical applications - Determination of airflow resistance", (1991).
- 20 Cox, T. and D'Antonio, P. Acoustic absorbers and diffusers, Spon Press, London, (2004).
- 21 Kirby, R. On the modification of Delany and Bazley formulae, Appl. Acoust., 86, 47-49, (2014).
- 22 Jeong, C.-H. Predicting the Sabine absorption coefficients of fibrous absorbers for various air backing conditions with a frequency-dependent diffuseness correction, J. Acoust. Soc. Am., 140, 1498-1501, (2016).